

SLIM: Semantic-based Low-bitrate Image compression for Machines by leveraging diffusion

Hyeonjin Lee

School of Integrated Technology, Yonsei University
Republic of Korea
hyeonjin.lee@yonsei.ac.kr

Jun-Hyuk Kim*

Department of Artificial Intelligence, Chung-Ang University
Republic of Korea
junhyukim@cau.ac.kr

Jong-Seok Lee*

School of Integrated Technology, Yonsei University
Republic of Korea
jong-seok.lee@yonsei.ac.kr

Abstract

In recent years, the demand of image compression models for machine vision has increased dramatically. However, the training frameworks of image compression still focus on the vision of human, maintaining the excessive perceptual details, thus have limitations in optimally reducing the bits per pixel in the case of performing machine vision tasks. In this paper, we propose Semantic-based Low-bitrate Image compression for Machines by leveraging diffusion, termed SLIM. This is a new effective training framework of image compression for machine vision, using a pre-trained latent diffusion model. The compressor model of our method focuses only on the Region-of-Interest (RoI) areas for machine vision in the image latent, to compress it compactly. Then the pretrained Unet model enhances the decompressed latent, utilizing a RoI-focused text caption which containing semantic information of the image. Therefore, SLIM is able to focus on RoI areas of the image without any guide mask at the inference stage, achieving low bitrate when compressing. And SLIM is also able to enhance a decompressed latent by denoising steps, so the final reconstructed image from the enhanced latent can be optimized for the machine vision task while still containing perceptual details for human vision. Experimental results show that SLIM achieves a higher classification accuracy in the same bits per pixel condition, compared to conventional image compression models for machines.

1. Introduction

As the demand of transmitting image data grows significantly, the methods of image compression have been studied consistently. From the traditional methods such as JPEG

[28] and JPEG2000 [22] to the end-to-end learned image compression models [2, 23] trained with the rate-distortion optimization, many studies have aimed to compress images to low bitrates while preserving essential information for high quality of reconstructed images.

However, the high quality of reconstructed images has been evaluated primarily based on human vision, how visually pleasing to humans. Thus, existing image compression models that reconstruct images with high perceptual quality often exhibit suboptimal performance when their reconstructed images are used for machine vision tasks. Although the share of compressed images processed by machines is increasing rapidly, research addressing this important issue remains limited.

Although several studies [7, 17, 18, 27, 32] have explored image compression for machine vision, existing approaches still exhibit clear limitations at low bit rates. While image compression for machine vision can tolerate reduced visual fidelity compared to human vision, pushing the bitrate too low often fails to preserve even the essential semantic information required for downstream machine vision task. Moreover, the degraded visual quality at low bitrates, such as block-wise noise and compression artifacts, further undermines task performance.

To address this issue, we propose SLIM, a Semantic-based Low-bitrate Image compression for Machines by leveraging diffusion. Our model employs two key strategies to perform robustly even at low bitrates: first, focusing on the Region-of-Interest (RoI) areas relevant to machine vision tasks, and second, leveraging a pretrained diffusion model with strong generative capability. By concentrating on RoI areas and aggressively removing features from non-RoI areas, the model is able to compress images effectively

while preserving important semantic information even under low bitrate conditions. Simultaneously, denoising steps of the diffusion model enhance the decompressed latent representations into refined latent features, thereby improving the quality of the reconstructed images. Our model is designed to control the diffusion model to better incorporate semantic information from ROI-focused captions during latent enhancement. As a result, SLIM is capable of compressing images to low bitrates while still reconstructing high-quality images that enable strong performance on the downstream machine vision task.

Our main contributions are as follows.

- We propose a novel framework of image compression for machines, SLIM, which employs a pretrained diffusion module to optimize reconstructed images for machine vision.
- Our approach effectively reduces the bitrate by focusing on ROI areas within the image for machine vision, allowing low bitrate compression without significant loss of important information.
- Our experimental results show that SLIM requires only a low bitrate to achieve the same classification accuracy as other image compression models for machines.

2. Related Works

2.1. Learned image compression

Traditional image compression methods [5, 9, 22, 28], such as JPEG and VVC, are simple and widely used, but their performance is limited by hand-crafted transforms and quantization schemes. Learned image compression (LIC) methods [2] have emerged to address these limitations by training neural networks in an end-to-end manner, demonstrating superior rate-distortion performance compared to conventional codecs. Their typical training objective is defined as a rate-distortion trade off:

$$\mathcal{L} = \mathcal{R} + \lambda \cdot \mathcal{D}(x, \hat{x}), \quad (1)$$

where x and \hat{x} denote the original and reconstructed images, $\mathcal{D}(x, \hat{x})$ is a distortion loss measuring reconstruction quality, \mathcal{R} is the estimated bitrate, and λ balances the trade-off between rate and distortion.

Recent studies further improve LIC models [3, 23, 33] using hyperprior models, autoregressive context models, or transformer-based architectures to enhance entropy modeling or capture long-range dependencies. Despite these advances, most existing approaches primarily focus on human visual perception, leaving challenges in scenarios with low bitrates.

2.2. Image compression for machine vision

The image compression models trained for human vision have the issue that their reconstructed images may not be

optimal for machine vision, thus showing a significant drop in performance when the reconstructed images are used in the downstream task like classification. To handle this issue, some studies have focused on the image compression models for machine vision.

There are the approaches [17, 27] that sacrifice the image quality, discarding background regions or features which are not necessary for machine vision, in order to leverage the efficiency benefits of the image compression for machines over the image compression for humans. To discard the specific region fidelity, it requires of feeding the hand-crafted mask into the model at the inference stage or utilizing a separate mask-generation model like SAM [16] at the training stage. Another approach [32], which trains the model for both human vision and machine vision simultaneously, achieves high fidelity while reconstructing the image suitable for machine vision but requires the cost for training multiple encoders. There are other approaches [7, 18] that convert the pretrained image compression for human vision into the model for machine vision by adjusting some part of the model weights or attaching the adapter modules to the model. Such methods are efficient to obtain the image compression model for machine vision, since they use the pretrained models for human vision and only train a limited set of weight parameters.

Instead of using the pretrained image compression models for human vision, our study utilizes the pretrained latent diffusion model to construct the improved image compression model for machine vision. And our framework SLIM aggressively removes unnecessary perceptual details required for human vision, leveraging the efficiency benefits of the image compression model for machine vision, but still reconstruct the high quality images by using the diffusion model.

2.3. Image compression with generative models

To maximize the quality of reconstructed images, several studies [1, 6, 11, 15, 29] have explored image compression methods based on generative models, such as GAN [10] or diffusion models [14, 25]. These approaches have achieved strong realism in reconstructed images by synthesizing details that other methods often lose, even at low bitrates. However, they still face limitations in maintaining fidelity under extreme compression. Moreover, existing methods have focused primarily on image compression for human perception. Motivated by these works, our study explores a diffusion-based image compression model for machine vision, which can better preserve the fidelity of ROI areas under low bitrates.

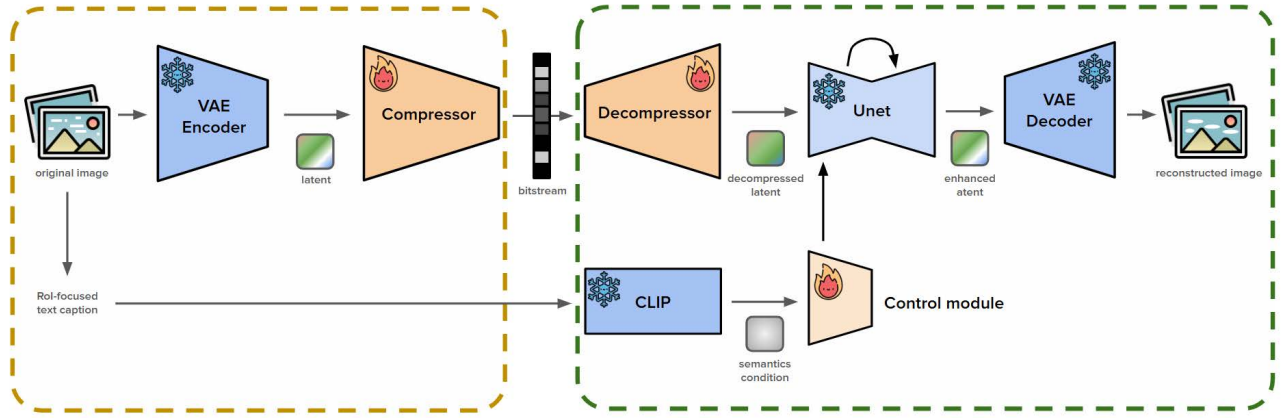


Figure 1. Architecture of SLIM. The weights of the fixed components are taken from Stable Diffusion.

3. Proposed method

3.1. System description

The overall architecture of our model is shown in Fig. 1. The encoder part consists of a VAE encoder and a compressor, and the decoder part includes a decompressor, a VAE decoder, CLIP encoder, Unet, and control module. We leverage pretrained components from Stable Diffusion 2.1, including the VAE encoder, VAE decoder, Unet, and CLIP encoder. The key trainable components of SLIM, however, are the compressor, the decompressor, and the control module. The compressor transforms the latent representation produced by the VAE encoder into a compact bitstream, while the decompressor reconstructs the latent from this bitstream. And the control module controls the Unet to incorporate RoI-focused semantic information into the enhanced latent. The overall architecture of our model is shown in Fig. 1.

During inference, an input image is first encoded into a latent representation by the VAE encoder. The compressor then transforms this latent into a bitstream, focusing on RoI areas, and this bitstream is transmitted to the decoder along with a RoI-focused text caption extracted from the image. In the decoder, the decompressor reconstructs the latent from the received bitstream. Before passing through the VAE decoder, the latent is enhanced by the Unet, which is conditioned on the RoI-focused text caption via the control module. The control module ensures that the Unet effectively incorporates RoI-focused semantic information into the latent representation, thereby improving the quality of the reconstructed image for downstream machine vision tasks.

3.2. Two-stage training

Since SLIM uses the pretrained diffusion model, Stable Diffusion 2.1 [25], only the compressor, the decompressor, and the control module need to be trained. The training phase of SLIM is divided into two stages, as shown in Fig. 2. In stage 1, the compressor-decompressor pair is trained to focus on RoI areas of machine vision, and the control module attached to the pretrained Unet is trained to reflect semantics provided in the form of text captions on the image latent. Then in stage 2, additional objectives are included in training, optimizing the reconstructed image samples for machine vision while maintaining natural textures. Details are as follows.

3.2.1. Stage 1

At first, the trainable components of SLIM are trained with RoI-focused approaches in the training stage 1. To enable the compressor and decompressor to focus on RoI areas when compressing and decompressing the image latent, we define the guide loss as follows:

$$\mathcal{L}_{\text{guide}} = \text{MSE}(\mathcal{M}_{\text{ROI}}(z), \mathcal{M}_{\text{ROI}}(\hat{z})) \quad (2)$$

where z and \hat{z} mean the latent encoded by the VAE encoder and the latent decompressed by the decompressor, respectively. $\mathcal{M}_{\text{ROI}}(\cdot)$ is the operation applying the RoI-mask to the input so that it focuses only on the RoI areas, and $\text{MSE}(\cdot, \cdot)$ is the mean squared errors between two inputs. In this study, the predefined RoI-mask used in the guide loss is obtained by the results of Grad-CAM [26] when the image samples pass the pretrained ResNet50 [13]. The RoI-mask corresponding to the image is resized to match the size of the latent to be masked. Therefore, when the compressor and decompressor are trained to compress and decompress

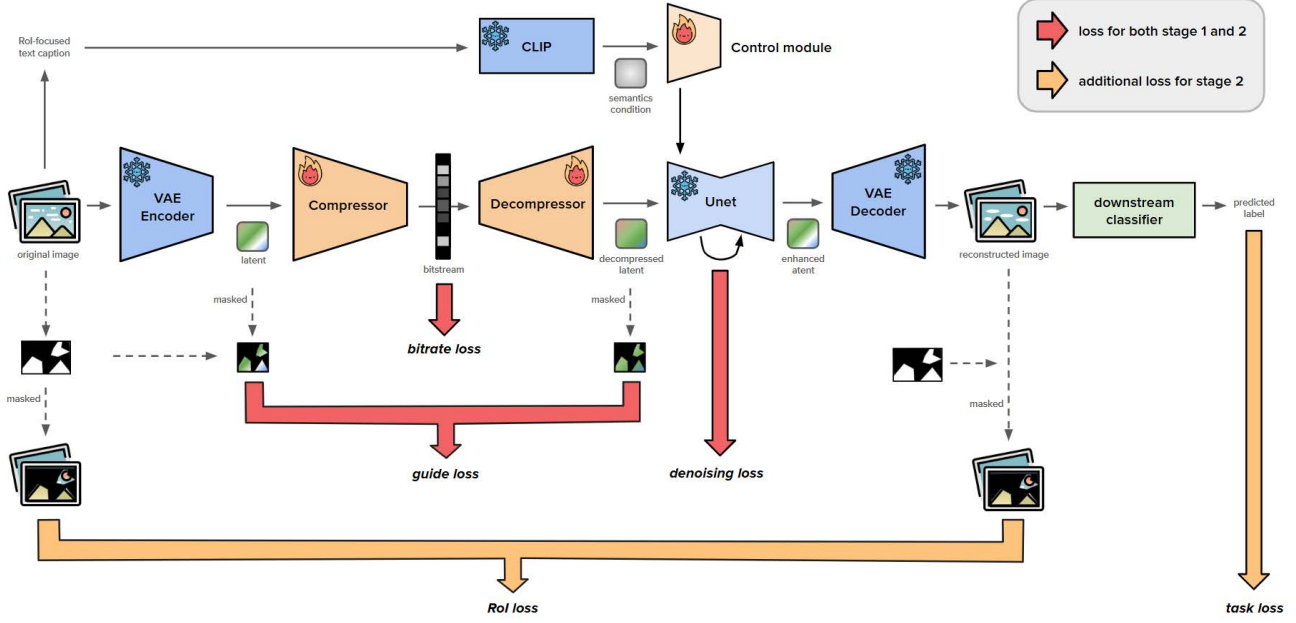


Figure 2. Procedure of two-stage training.

the image latent, the fidelity is only calculated on the RoI areas where the machine vision shows high attention. With the bitrate loss \mathcal{R} , SLIM is trained to reduce more bits on non-RoI areas where fidelity is less critical.

Besides, for training the control module attached to the pretrained Unet, we define the denoising loss as follows:

$$\mathcal{L}_{denoise} = MSE(\epsilon, \epsilon_\theta(z_t, t, c)) \quad (3)$$

where ϵ is the target noise and ϵ_θ is the predicted noise by the Unet attached with the control module with weight parameters θ . The Unet predict ϵ_θ from the noisy latent z_t at the timestep t , with the semantics condition c . The semantics condition c is the CLIP [24] embedded text captions which are the results of image captioning by the vision-language model (VLM), such as LLaVA [20] and BLIP2 [19]. For obtaining RoI-focused semantics, we use the image with RoI-mask applied as the input of BLIP2 for image captioning.

Thus, the loss function of the training stage 1 is formulated as follows:

$$\mathcal{L}_{stage1} = \lambda_r \cdot \mathcal{R} + \lambda_g \cdot \mathcal{L}_{guide} + \lambda_d \cdot \mathcal{L}_{denoise} \quad (4)$$

where λ_r , λ_g , and λ_d are hyperparameters to balance the losses.

3.2.2. Stage 2

Based on \mathcal{L}_{stage1} , additional losses are included in the training stage 2. To ensure the reconstructed image samples

maintain the fidelity and semantics of RoI areas in original images, we define the RoI loss as follows:

$$\begin{aligned} \mathcal{L}_{ROI} = & MSE(\mathcal{M}_{ROI}(x), \mathcal{M}_{ROI}(\hat{x})) \\ & + LPIPS(\mathcal{M}_{ROI}(x), \mathcal{M}_{ROI}(\hat{x})) \end{aligned} \quad (5)$$

where $LPIPS(\cdot, \cdot)$ means the LPIPS loss [31] between two inputs. The first term $MSE(\mathcal{M}_{ROI}(x), \mathcal{M}_{ROI}(\hat{x}))$ is the mean squared error between the original image x and reconstructed image \hat{x} in RoI areas, for high fidelity of RoI areas in reconstructed images at the pixel level. And the second term $LPIPS(\mathcal{M}_{ROI}(x), \mathcal{M}_{ROI}(\hat{x}))$ is the LPIPS loss between the original image x and reconstructed image \hat{x} in RoI areas, for high perceptual details of RoI areas in reconstructed images at the semantics level.

To ensure the reconstructed image samples are optimized for machine vision, we define the task loss as follows:

$$\mathcal{L}_{task} = CE(y, \hat{y}) \quad (6)$$

where y and \hat{y} are the ground truth class label and the predicted class label respectively, and $CE(\cdot, \cdot)$ means the cross-entropy loss between two inputs. The predicted class label \hat{y} is obtained by feeding the reconstructed image into the classifier model.

Thus, the loss function of the training stage 2 is formulated as follows:

$$\mathcal{L}_{stage2} = \mathcal{L}_{stage1} + \lambda_{ROI} \cdot \mathcal{L}_{ROI} + \lambda_t \cdot \mathcal{L}_{task} \quad (7)$$

where λ_{ROI} and λ_t are hyperparameters to balance the losses.

3.3. Inference

After two training stages, the trained SLIM works on the following scheme. First, the image is encoded into the latent by the VAE encoder. Then, the latent is compressed into a bitstream via the compressor, and decompressed back to the latent. Note that the decompressed latent from the decompressor is the ROI-focused latent, even though we never feed the ROI-mask or other information demonstrating where are the ROI areas of the image to the compressor. Before decoding this ROI-focused latent to the image, it is enhanced by denoising steps of the text-conditional diffusion model. At last, the enhanced latent is decoded to the reconstructed image by the VAE decoder. This reconstructed image, though strongly compressed at a low bitrate, still results in a high performance when it is used in the downstream machine vision task, classification.

4. Experimental results

4.1. Experimental setup

We conduct experiments and analyses to evaluate SLIM in comparison with pretrained image compression models from prior studies. And further, we analyze how each component of SLIM affects the performance of the model, through ablation studies. Details of training settings, datasets, and comparison models used in experiments are provided below.

Training setup. We train our SLIM model for 100,000 steps in stage 1 and 100,000 steps in stage 2. The AdamW is employed as the optimizer, and the learning rate is set to 0.0001. We randomly select 3,000 image samples from ImageNet-train [8] dataset, then construct a dataset for model training, which consists of image samples, their ROI-mask and ROI-focused text captions.

Comparison. The pretrained models from prior studies used as comparison models are as follows: SA-ICM [27], which is trained from scratch for machine vision; TransTIC [7] and AdaptICMH [18], which are transferred or adapted for machine vision from the base models trained for human vision; and MPA [32], trained to be applicable to both human vision and various machine vision tasks. We also use the pretrained model of OSCAR [11], which is a state-of-the-art model trained for human vision, as an additional comparison model to compare in terms of learned image compression models using diffusion models. We evaluate the rate-accuracy performance on the ImageNet-val dataset. To assess the classification accuracy, we employ classifier models including ResNet50 [13] or ConvNeXt-T [21] on the reconstructed image samples.

Table 1. BD-Rate comparison on the ImageNet-val dataset.

Model	ResNet50 (%) ↓	ConvNeXt-T (%) ↓
MPA	-	-
TransTIC	-67.23	-55.16
AdaptICMH	-75.60	-65.14
OSCAR	-90.89	-87.26
SLIM (Ours)	-94.56	-91.73

4.2. Rate-accuracy performance

As shown in Fig. 3, our SLIM model achieves the best rate-accuracy performance compared to other baselines when evaluated with both ResNet50 and ConvNeXt-T classifiers. In comparison with the models for machine vision, including MPA, TransTIC, AdaptICMH, our approach requires consistently fewer bits per pixel (bpp) to achieve the same classification accuracy. This demonstrates the higher coding efficiency of SLIM. Furthermore, in comparison with the model for human vision, OSCAR, our approach still achieves better rate-accuracy performance. Particularly at low bitrates, SLIM maintains reasonable accuracy while OSCAR shows a significant drop in accuracy. This suggests that although both SLIM and OSCAR utilize the diffusion model, SLIM is specially designed for machine vision and its effectiveness is increasingly noticeable when a compression ratio increases. The corresponding BD-Rate comparison results are reported in Tab. 1. We compute the BD-Rate (Bjøntegaard delta rate) according to the method proposed by Bjøntegaard [4], measuring the average bitrate difference between two rate-accuracy (bpp vs Top-1 Acc) curves via cubic interpolation. A negative BD-Rate value means the image compression model is more efficient than the reference model. Compared to MPA model, SLIM achieves an average BD-Rate reduction of -94.56 % and -91.73 %, with ResNet50 and ConvNeXt-T classifier respectively, on the ImageNet-val dataset.

4.3. Qualitative results

To further demonstrate the reconstructed image quality of SLIM, we also conduct a qualitative comparison with other learned image compression models. We compare our model with AdaptICMH, TransTIC, MPA. Fig. 4 shows reconstructed image samples from each learned image compression model at comparable bpp levels. Our method reconstructs the images with more natural textures than others, particularly in the ROI areas for machine vision. While other models tend to lose texture and details in reconstructed image at low bitrates, our SLIM model strategically removes details only in non-ROI areas and preserves the crucial texture and details in ROI areas of the image. This leads to our model achieving the high classification accuracy per-

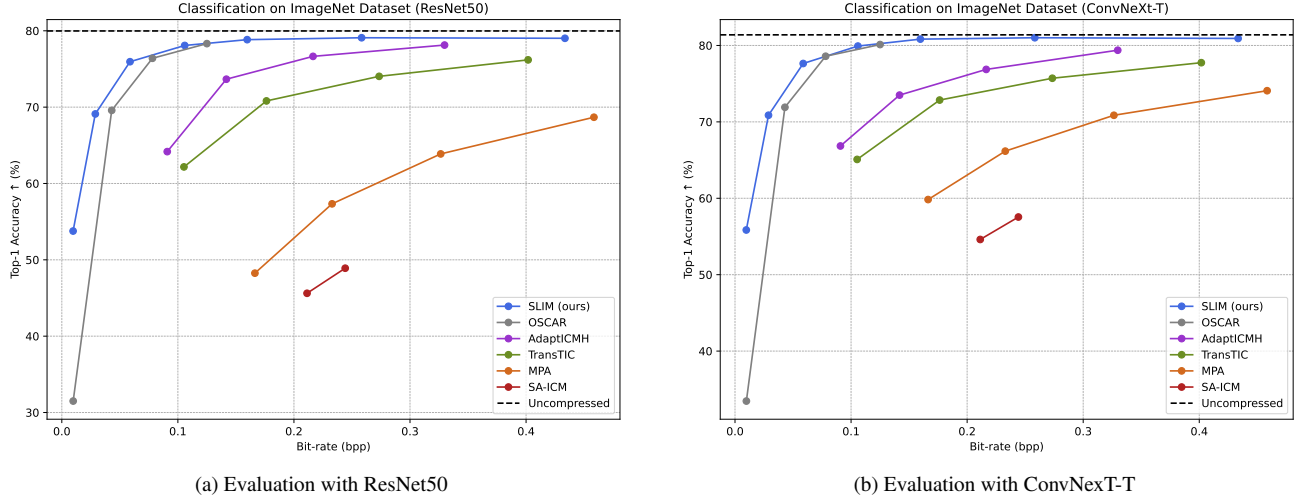


Figure 3. Rate-accuracy performance comparison results. We evaluate classification accuracy on the ImageNet-val dataset by passing reconstructed images from each learned image compression model through machine vision classifiers, ResNet50 and ConvNeXt-T.

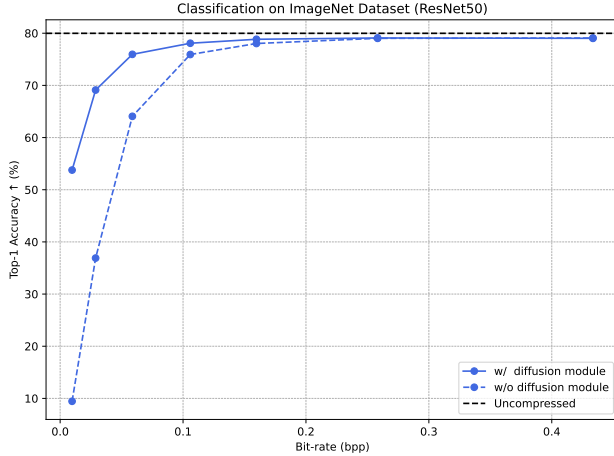


Figure 4. Reconstructed samples from different models, AdaptICMH [18], TransTIC [7], MPA [32], and Ours.

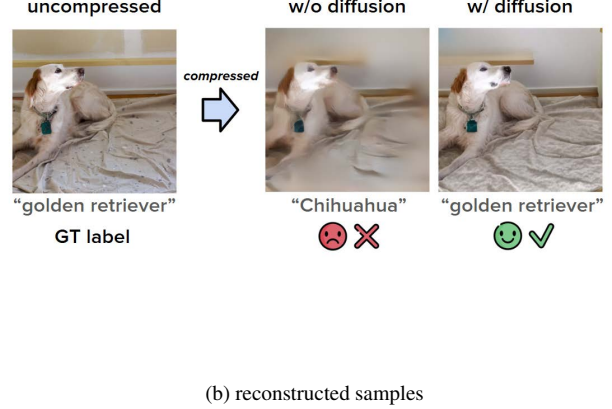
formance in low bitrates. And also the results of this qualitative comparison, confirming that the image reconstructed by using diffusion contains more natural textures and better quality, support the superior rate-accuracy performance of SLIM.

4.4. Ablation studies

Through ablation studies, we compare the results of image reconstruction with and without denoising steps of Unet, and examine how the bit allocation maps of the compressor



(a) rate-accuracy comparison



(b) reconstructed samples

Figure 5. Comparison between SLIM models with and without the diffusion module.

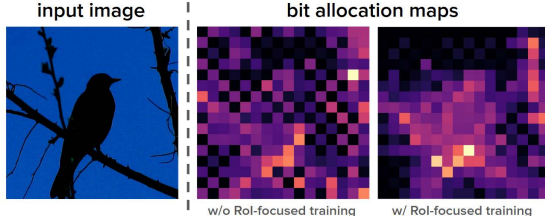


Figure 6. Bit allocation maps comparison. We obtain the bit allocation maps from SLIM models with and without ROI-focused training.

changes with and without the ROI-focused training strategy.

Diffusion module. As shown in Fig. 5a, the diffusion module has a significant impact on the rate-accuracy performance of SLIM. Compared to the case without the diffusion module, our SLIM model with the diffusion module achieves higher accuracy at the same bitrate level, especially in low bitrates. Without the diffusion module, no denoising steps of Unet for enhancing the image latent is involved before passing it to the VAE decoder, and the non-enhanced latent which decompressed by decompressor are directly used to be decoded by the VAE decoder. Then the image samples reconstructed from the imperfect latent are imperfect for both human vision and machine vision, due to the aggressive compression approach of the compressor (Fig. 5b). The diffusion module is a crucial component that enhances the imperfect latent into the latent with rich semantics and details, through denoising steps of Unet. Since the compressor removes more information of the latent, thus the effect of latent enhancement via diffusion model is increased in low bitrates.

ROI-focused training. To confirm that the compressor

Table 2. BD-Rate comparison on the ImageNet-val dataset with ResNet50 classifier.

Model	BD-Rate (%) ↓
w/o ROI-focused training	-
w/ ROI-focused training	-18.87

of SLIM focuses on the ROI areas in the latent as intended, we observe the bit allocation maps of SLIM. Fig. 6 represents the bit allocation maps from SLIM models after the training stage 1, with and without ROI-focused training. The SLIM model without ROI-focused training adopts a modified guide loss, computed on a full area of the image latent without ROI-mask. While the bit allocation map obtained from the SLIM model without ROI-focused training relatively exhibits a more uniform bit distribution, the SLIM model with ROI-focused training shows a higher concentration of bits on ROI areas for machine vision. We also confirm that this intended ROI-focused strategy leads the higher BD-Rate performance as shown in Tab. 2. Employing ROI-focused training results in a BD-rate reduction of 18.87%.

5. Conclusion

In this paper, we proposed a novel semantic-based framework of learned image compression for machine vision, named SLIM. Our SLIM model could efficiently reduce the bitrate by the compressor focusing on the ROI areas of the image latent, and effectively improve the quality of a reconstructed image by the diffusion module enhancing the decompressed latent through denoising steps. This work provides a novel scheme for learned image compression in machine vision applications, utilizing ROI-focused training and pretrained diffusion. Experi-

iments showed that SLIM outperforms the other existing learned image compression models, in rate-accuracy performance and reconstructed quality. In future work, we aim to accelerate our model by utilizing an one-step diffusion.

References

- [1] Eirikur Agustsson, Michael Tschannen, Fabian Mentzer, Radu Timofte, and Luc Van Gool. Generative adversarial networks for extreme learned image compression. In *Proceedings of the IEEE/CVF international conference on computer vision*, pages 221–231, 2019. [2](#)
- [2] Johannes Ballé, Valero Laparra, and Eero P Simoncelli. End-to-end optimized image compression. *arXiv preprint arXiv:1611.01704*, 2016. [1, 2](#)
- [3] Johannes Ballé, David Minnen, Saurabh Singh, Sung Jin Hwang, and Nick Johnston. Variational image compression with a scale hyperprior. *arXiv preprint arXiv:1802.01436*, 2018. [2](#)
- [4] Gisle Bjøntegaard. Calculation of average psnr differences between rd-curves. 2001. [5](#)
- [5] Benjamin Bross, Ye-Kui Wang, Yan Ye, Shan Liu, Jianle Chen, Gary J Sullivan, and Jens-Rainer Ohm. Overview of the versatile video coding (vvc) standard and its applications. *IEEE Transactions on Circuits and Systems for Video Technology*, 31(10):3736–3764, 2021. [2](#)
- [6] Marlene Careil, Matthew J Muckley, Jakob Verbeek, and Stéphane Lathuilière. Towards image compression with perfect realism at ultra-low bitrates. In *The Twelfth International Conference on Learning Representations*, 2023. [2](#)
- [7] Yi-Hsin Chen, Ying-Chieh Weng, Chia-Hao Kao, Cheng Chien, Wei-Chen Chiu, and Wen-Hsiao Peng. Transtic: Transferring transformer-based image compression from human perception to machine perception. In *Proceedings of the IEEE/CVF International Conference on Computer Vision*, pages 23297–23307, 2023. [1, 2, 5, 6](#)
- [8] Jia Deng, Wei Dong, Richard Socher, Li-Jia Li, Kai Li, and Li Fei-Fei. Imagenet: A large-scale hierarchical image database. In *Proceedings of the IEEE/CVF Conference on Computer Vision and Pattern Recognition (CVPR)*, pages 248–255, 2009. [5](#)
- [9] Bellard Fabrice. Bpg image format. <https://bellard.org/bpg/>, 2014. [2](#)
- [10] Ian Goodfellow, Jean Pouget-Abadie, Mehdi Mirza, Bing Xu, David Warde-Farley, Sherjil Ozair, Aaron Courville, and Yoshua Bengio. Generative adversarial networks. *Communications of the ACM*, 63(11):139–144, 2020. [2](#)
- [11] Jinpei Guo, Yifei Ji, Zheng Chen, Kai Liu, Min Liu, Wang Rao, Wenbo Li, Yong Guo, and Yulun Zhang. Oscar: One-step diffusion codec across multiple bit-rates. *arXiv preprint arXiv:2505.16091*, 2025. [2, 5](#)
- [12] Dailan He, Ziming Yang, Weikun Peng, Rui Ma, Hongwei Qin, and Yan Wang. Elic: Efficient learned image compression with unevenly grouped space-channel contextual adaptive coding. In *Proceedings of the IEEE/CVF conference on computer vision and pattern recognition*, pages 5718–5727, 2022. [1](#)
- [13] Kaiming He, Xiangyu Zhang, Shaoqing Ren, and Jian Sun. Deep residual learning for image recognition. In *Proceedings of the IEEE/CVF Conference on Computer Vision and Pattern Recognition (CVPR)*, pages 770–778, 2016. [3, 5](#)
- [14] Jonathan Ho, Ajay Jain, and Pieter Abbeel. Denoising diffusion probabilistic models. *Advances in neural information processing systems*, 33:6840–6851, 2020. [2](#)
- [15] Anle Ke, Xu Zhang, Tong Chen, Ming Lu, Chao Zhou, Jiawen Gu, and Zhan Ma. Ultra lowrate image compression with semantic residual coding and compression-aware diffusion. *arXiv preprint arXiv:2505.08281*, 2025. [2](#)
- [16] Alexander Kirillov, Eric Mintun, Nikhila Ravi, Hanzi Mao, Chloe Rolland, Laura Gustafson, Tete Xiao, Spencer Whitehead, Alexander C Berg, Wan-Yen Lo, et al. Segment anything. In *Proceedings of the IEEE/CVF international conference on computer vision*, pages 4015–4026, 2023. [2](#)
- [17] Binglin Li, Jie Liang, Haisheng Fu, and Jingning Han. Roi-based deep image compression with swin transformers. In *ICASSP 2023-2023 IEEE International Conference on Acoustics, Speech and Signal Processing (ICASSP)*, pages 1–5, 2023. [1, 2](#)
- [18] Han Li, Shaohui Li, Shuangrui Ding, Wenrui Dai, Maida Cao, Chenglin Li, Junni Zou, and Hongkai Xiong. Image compression for machine and human vision with spatial-frequency adaptation. In *European Conference on Computer Vision*, pages 382–399, 2024. [1, 2, 5, 6](#)
- [19] Junnan Li, Dongxu Li, Silvio Savarese, and Steven Hoi. Blip-2: Bootstrapping language-image pre-training with frozen image encoders and large language models. In *International conference on machine learning*, pages 19730–19742, 2023. [4, 1](#)
- [20] Haotian Liu, Chunyuan Li, Qingyang Wu, and Yong Jae Lee. Visual instruction tuning. *Advances in neural information processing systems*, 36:34892–34916, 2023. [4](#)
- [21] Zhuang Liu, Hanzi Mao, Chao-Yuan Wu, Christoph Feichtenhofer, Trevor Darrell, and Saining Xie. A convnet for the 2020s. In *Proceedings of the IEEE/CVF conference on computer vision and pattern recognition*, pages 11976–11986, 2022. [5](#)
- [22] Michael W Marcellin, Michael J Gormish, Ali Bilgin, and Martin P Bolek. An overview of jpeg-2000. In *Proceedings DCC 2000. Data compression conference*, pages 523–541, 2000. [1, 2](#)
- [23] David Minnen, Johannes Ballé, and George D Toderici. Joint autoregressive and hierarchical priors for learned image compression. *Advances in neural information processing systems*, 31, 2018. [1, 2](#)
- [24] Alec Radford, Jong Wook Kim, Chris Hallacy, Aditya Ramesh, Gabriel Goh, Sandhini Agarwal, Girish Sastry, Amanda Askell, Pamela Mishkin, Jack Clark, et al. Learning transferable visual models from natural language supervision. In *International conference on machine learning*, pages 8748–8763. PMLR, 2021. [4](#)
- [25] Robin Rombach, Andreas Blattmann, Dominik Lorenz, Patrick Esser, and Björn Ommer. High-resolution image synthesis with latent diffusion models. In *Proceedings of the IEEE/CVF conference on computer vision and pattern recognition*, pages 10684–10695, 2022. [2, 3](#)

- [26] Ramprasaath R Selvaraju, Michael Cogswell, Abhishek Das, Ramakrishna Vedantam, Devi Parikh, and Dhruv Batra. Grad-cam: Visual explanations from deep networks via gradient-based localization. In *Proceedings of the IEEE/CVF International Conference on Computer Vision (ICCV)*, pages 618–626, 2017. [3](#)
- [27] Takahiro Shindo, Kein Yamada, Taiju Watanabe, and Hiroshi Watanabe. Image coding for machines with edge information learning using segment anything. In *2024 IEEE International Conference on Image Processing (ICIP)*, pages 3702–3708, 2024. [1](#), [2](#), [5](#)
- [28] Gregory K Wallace. The jpeg still picture compression standard. *Communications of the ACM*, 34(4):30–44, 1991. [1](#), [2](#)
- [29] Ruihan Yang and Stephan Mandt. Lossy image compression with conditional diffusion models. *Advances in Neural Information Processing Systems*, 36:64971–64995, 2023. [2](#)
- [30] Tianwei Yin, Michaël Gharbi, Richard Zhang, Eli Shechtman, Fredo Durand, William T Freeman, and Taesung Park. One-step diffusion with distribution matching distillation. In *Proceedings of the IEEE/CVF conference on computer vision and pattern recognition*, pages 6613–6623, 2024. [2](#)
- [31] Richard Zhang, Phillip Isola, Alexei A Efros, Eli Shechtman, and Oliver Wang. The unreasonable effectiveness of deep features as a perceptual metric. In *Proceedings of the IEEE conference on computer vision and pattern recognition*, pages 586–595, 2018. [4](#)
- [32] Xu Zhang, Peiyao Guo, Ming Lu, and Zhan Ma. All-in-one image coding for joint human-machine vision with multi-path aggregation. *Advances in Neural Information Processing Systems*, 37:71465–71503, 2024. [1](#), [2](#), [5](#), [6](#)
- [33] Yinhao Zhu, Yang Yang, and Taco Cohen. Transformer-based transform coding. In *International conference on learning representations*, 2022. [2](#)

SLIM: Semantic-based Low-bitrate Image compression for Machines by leveraging diffusion

Supplementary Material

6. ROI-focused text captions

To obtain ROI-focused text captions, we feed the ROI-masked image into BLIP2 [19], which generates a description of the preserved areas. Samples of the resulting ROI-focused text captions are shown in Fig. 7. The ROI-focused text captions after compression with the zlib lossless compression algorithm require only 367 bits on average. For comparison with the bitrate of compressed images, we normalize the ROI-focused caption bits by the number of pixels in the image ($512 \times 512 = 262,144$ pixels). On this scale, the captions require only 0.0014 bpp on average, which is extremely small compared to the bitrate required for the compressed image data.

original image	ROI-focused image	ROI-focused text caption	bits (bpp)
		"a dog with a bone in its mouth"	304 (0.0012)
		"three yellow bowls with green floral designs on them"	456 (0.0017)
		"a red barn in the middle of a field"	344 (0.0013)
		"a large sailboat is sailing on the water"	352 (0.0013)

Figure 7. Samples of the ROI-focused text captions for the ImageNet-val dataset.

7. Training on an extended dataset

We examine the effect of the training dataset size. For this, we additionally train our SLIM model on an extended dataset constructed by combining OpenImages v6 (train), CLIC2020 professional (train), and COCO2017 (train), which comprises of approximately 170,000 images. Since this extended dataset does not include the ground-truth labels required for computing the task loss in training stage 2, we train the model only up to training stage 1. Fig. 8 shows the performance comparison between the model trained on the 170K images from the extended dataset and the model trained on 3,000 images from the ImageNet-train dataset.

The experimental result indicates that our SLIM model has the potential to achieve better classification accuracy at low bitrates when trained on extended datasets.

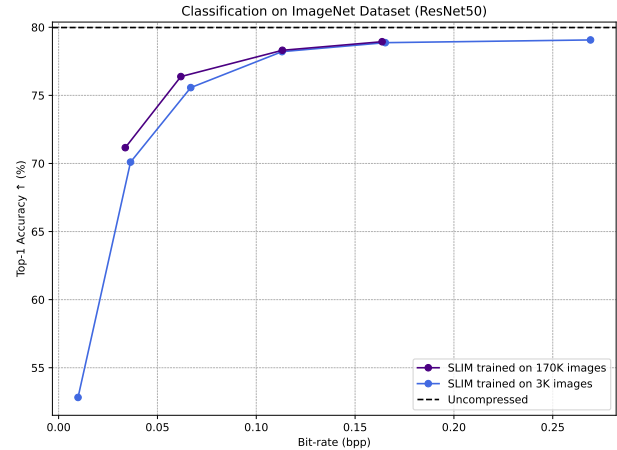


Figure 8. Comparison between the SLIM models trained on datasets of different sizes up to training stage 1.

8. Details of compressor-decompressor pair

Inspired by the ELIC [12] framework for image compression, the compressor-decompressor pair of our SLIM applies hyperprior-based compression on the latent produced by the VAE encoder, using a checkerboard slicing strategy. The pair consists of a latent analysis transform, hyper analysis transform, hyper synthesis transform, and latent synthesis transform. The detailed structure of the pair models is shown in Fig. 9.

The compressor first applies the latent analysis transform to the input latent, producing the compressed features. Then, the hyper analysis transform extracts hyper features from these compressed features to support entropy coding. During entropy-coding, the compressed features are divided into multiple slices, which are processed sequentially using a checkerboard-channel context.

On the decompressor side, the hyper synthesis transform produces the distribution parameters from the hyper features, leveraging the checkerboard-channel context to better estimate those parameters for entropy-decoding each slice of the compressed features. Finally, the latent synthesis transform reconstructs the output latent from the decompressed features.

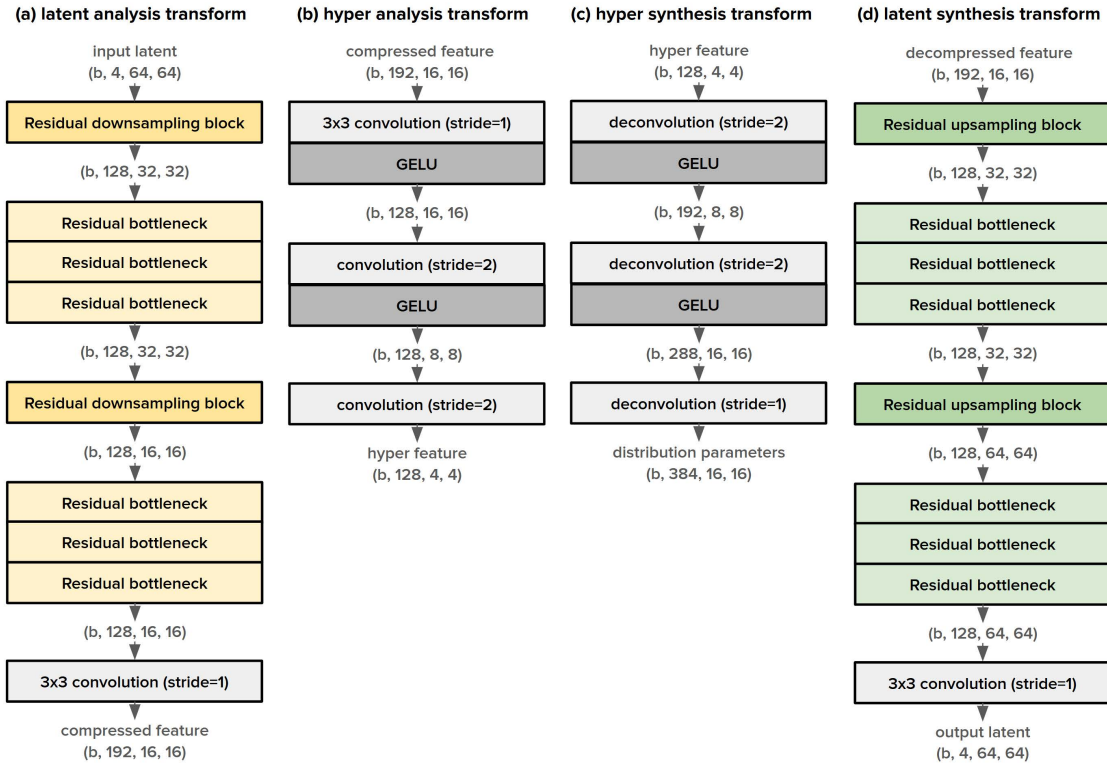


Figure 9. Architecture of the compressor-decompressor pair of SLIM. Each residual bottleneck consists of three convolution layers and two GELU layers with a residual connection, whereas the residual downsampling and upsampling blocks consists of three convolution layers and two leaky ReLU layers, also with a residual connection.

9. Computational efficiency

We analyze the computational cost of our SLIM model. As shown in Table 3, processing a 512×512 sized RGB image takes a total of 1657.83 GFLOPs. Specifically, the encoding phase requires 575.61 GFLOPs, while the decoding takes 1082.22 GFLOPs, indicating that the majority of the computational cost arises from the diffusion module in the decoding phase. Thus, our method yields improved rate-accuracy performance at the cost of increased computational complexity compared with non-diffusion based approaches. In addition, our method achieves a decoding time comparable to OSCAR [11] while requiring only about two-thirds of its GFLOPs, demonstrating higher computational efficiency than this diffusion-based baseline. The overall complexity could be further reduced by employing a one-step diffusion model [30].

10. Additional reconstructed images

This section presents further qualitative results of our SLIM model. Fig. 10 shows reconstructed images at comparable bpp levels.

Table 3. Computational cost of each model for a 512×512 sized RGB image. All latency values (ms) are obtained under a single NVIDIA RTX 4090 GPU setting.

Model	Encoding (GFLOPs / ms)	Decoding (GFLOPs / ms)
SA-ICM [27]	204.60 / 52.89	262.51 / 25.13
MPA [32]	45.68 / 20.88	80.69 / 84.69
TransTIC [7]	83.94 / 54.96	49.11 / 51.71
AdaptICMH [18]	38.64 / 36.20	50.11 / 39.77
OSCAR [11]	564.10 / 47.88	1591.33 / 182.69
SLIM (Ours)	575.61 / 50.60	1082.22 / 212.95

11. Additional samples from ablation studies

This section provides additional samples for the ablation studies. Fig. 11a shows reconstructed images comparing the SLIM models with and without the diffusion module, and Fig. 11b shows the bit allocation maps obtained from the SLIM models with and without ROI-focused training.

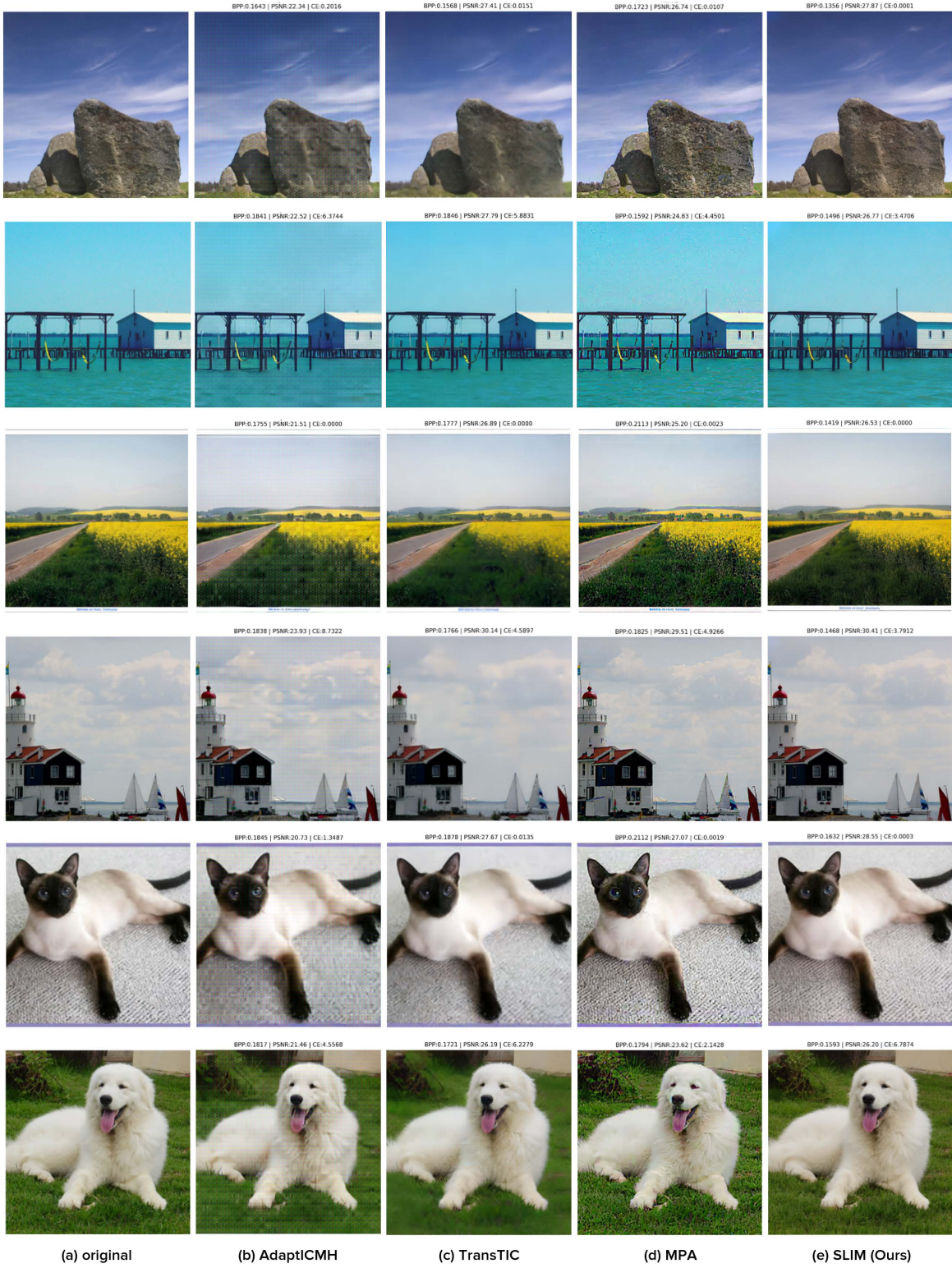
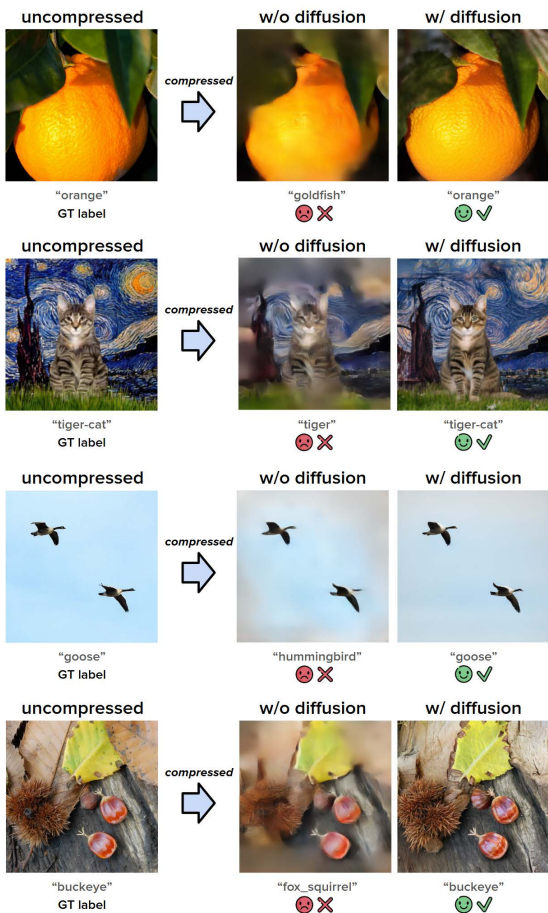
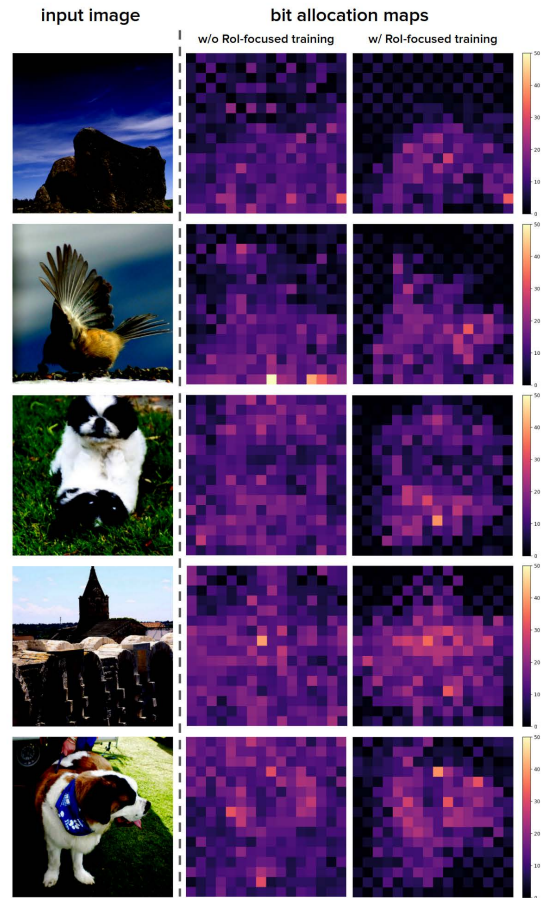


Figure 10. Reconstructed images from our SLIM model at comparable bpp levels.



(a) Reconstructed images with and without the diffusion module



(b) Bit allocation maps with and without ROI-focused training

Figure 11. Comparison between the SLIM models with and without (a) the diffusion module, and (b) ROI-focused training.